We are IntechOpen, the world's leading publisher of Open Access books Built by scientists, for scientists

6,900
Open access books available

186,000
International authors and editors

200M
Downloads

Our authors are among the

154
Countries delivered to

TOP 1%
most cited scientists

12.2%
Contributors from top 500 universities

WEB OF SCIENCE™

Selection of our books indexed in the Book Citation Index in Web of Science™ Core Collection (BKCI)

Interested in publishing with us?
Contact book.department@intechopen.com

Numbers displayed above are based on latest data collected.
For more information visit www.intechopen.com

18

From Local Interactive Measurements to Global Matrix Representations on Variant Construction – A Particle Model of Quantum Interactions for Double Path Experiments

Jeffrey Zheng[1], Christian Zheng[2] and T.L. Kunii[3]
[1]*Yunnan University*
[2]*University of Melbourne*
[3]*University of Tokyo*
[1]*P.R. China*
[2]*Australia*
[3]*Japan*

1. Introduction

1.1 Wave and particle duality in quantum measurements

Right from the introduction of Plank's modern quantum concept, measurement effects have played a central role in both theoretical and experimental considerations [Jammer (1974)]. Einstein (1916) photon effects favor a particle based explanation. de Broglie (1923) proposed wave and particle duality. Heisenberg proposed a matrix approach to handling complex operations based on spectra measurements. Schrödinger established a wave equation for quantum construction extending de Broglie's schemes. von Neumann (1932,1996)'s contribution placed quantum mechanics in Hilbert space to establish a solid mathematical foundation for modern quantum mechanics. Despite developments in the quantum approach spanning more than a century, fundamental measurement problems remain unsolved [Penrose (2004)]. All their lives, Bohr and Einstein engaged in many debates, discussions and arguments trying to reach a common understanding on wave and particle issues [Jammer (1974)]. The EPR (Einstein, Podolsky, Rosen) Paradox [Einstein et al. (1935)] is said to have given Bohr many sleepless nights [Bohr (1935; 1949)].

1.2 Criteria conditions and modern experiments

Quantum measurement puzzles have been explored by [Feynman (1965); Feynman et al. (1965,1989)]. From the 1940s, Feynman emphasized that: "The entire mystery of quantum mechanics is in the double-slit experiment." This experiment establishes an interactive model that can directly illustrate both classical and quantum interactive results. Under single and double slit conditions, dual visual distributions are shown in particle and wave statistical distributions. Both particle probability and wave interactive interference patterns are observed [Barnett (2009); Hawking & Mlodinow (2010); Healey et al. (1998)].

1.3 Modern experiments

Mach-Zehnder interferometers and Stern-Gerlach spin-devices play a key role in Quantum measurement development [Barnett (2009); Barrow et al. (2004); Hawking & Mlodinow (2010); Jammer (1974)]. Wave particle-duality has been demonstrated in larger particles [Arndt et al. (1999)] and advanced optical fibers, communication, computer software, photonics, and integrated technologies have been applied to different quantum media [Barrow et al. (2004); Grangier et al. (1986)].

1.3.1 Bell approaches

In the 1960s, Bell played an important role in exploring the foundations of the quantum approach [Bell (1964)]. Based on the EPR paradox, he proposed inequations for measurable experiments to distinguish between Bohr's Principle of Complementarity and Einstein's EPR paradox under a local realism framework [Aspect et al. (1982); Bell (2004)].

1.3.2 Advanced experiments

By the 1970s, work piloted by [Clauser et al. (1969)], Aspect et al. (1982) was using an experimental approach to test Bell Inequalities and to clearly show a significant gap between Bell Inequalities and real quantum reality.

After 40 years of development, many accurate experiments [Lindner et al. (2005); Zeh (1970); Zeilinger et al. (2005)] have been performed successfully worldwide using Laser, NMRI, large molecular, quantum coding and quantum communication approaches [Afshar et al. (2007); Barrow et al. (2004); Fox (2006); Merali (2007); Schleich et al. (2007)]. Following the application of advanced technologies and simulation methodologies, detailed single and multiple photon detection technologies have been further developed.

1.3.3 Weakness

However it does not matter how successful any single experiment or indeed many experiments might be, those results cannot simply replace the idea experiment of [Feynman et al. (1965,1989); Hawking & Mlodinow (2010); Penrose (2004)]. From a theoretical viewpoint, modern experiments involving Bell Inequations are excellent in illustrating the fundamental differences between a local realism and quantum reality. Since both theoretical and experimental activities focused on supporting or disproving Bell Inequalities cannot on their own provide a full explanation, further investigations are essential to provide a sound foundation on which a full understanding of quantum issues can be constructed.

1.4 From local interactive measurements to global matrix representations

In this chapter, a double path model has been established using the Mach-Zehnder interferometer. Different approaches to quantum measurements taken by Einstein, Stern-Gerlach, CHSH and Aspect are investigated to form quaternion structures. Using multiple-variable logic functions and variant principles, logic functions can be transferred into variant logic expressions as variant measures. Under such conditions, a variant simulation and representation model is proposed.

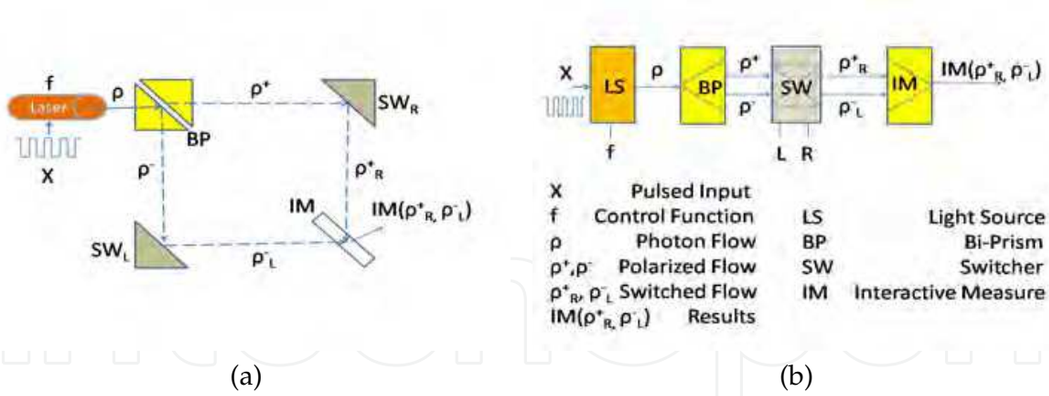

(a) (b)

Fig. 1. (a-b) Double Path Model (a) Mach-Zehnder Double Path Model (b) Description Model

A given logic function f, can be represented as two meta logic functions f_+ and f_- to simulate single and double path conditions. N bits of input vectors are exhausted by 2^N states for measured data, recursive data are organized into eight histograms. Results are determined by symmetry/anti-symmetry properties in histograms. All 2^{2^n} functions are applied to generate a set of histograms. Eight sets of histograms are represented as eight matrices in a selected C code configuration. Under this construction, it is possible to visualize different combinations from symmetry and anti-symmetry categories.

From these results, both additive probability properties in particle condition and wave interference properties with non-addition behaviors are observed. Both types of result are obtained consistently from this model under synchronous/asynchronous conditions. From a simulation viewpoint, this system satisfies all of Feynman's criteria conditions for double slit experiments.

2. Double path model and measurements of quantum interaction

2.1 Mach-Zehnder interferometer model

The Mach-Zehnder interferometer is the most popular device used to support a Young double slit experiment.

In Fig 1(a) a double path interferometer is shown. An input signal X under control function f causes Laser LS to emit the output signal ρ under BP (Bi-polarized filter) operation. The output is in the form of a pair of signals: ρ^+ and ρ^-. Both signals are processed by SW output ρ_L^+ and ρ_R^-, and then IM to generate output signals $IM(\rho_L^+, \rho_R^-)$. In Fig 1(b), a representation model has been described with the same signals being used.

2.1.1 Other devices

A Stern-Gerlach spin measurement device provides equivalent information for double path experiment [Jacques et al. (2008); Jammer (1974)]. This device divides composed signals into vertical $\perp$ and horizontal $\parallel$ components, in BP part $\rho \rightarrow \{\rho^\perp, \rho^\parallel\}$, through controls and IM output $IM(\rho_L^\perp, \rho_R^\parallel)$.

2.2 Emission and absorption measurements of quantum interaction

2.2.1 Einstein measurements

Einstein (1916) established the first model to describe atomic interaction with radiation. For two-state systems, Einstein's model is as follows. Let a system have two energy states: the ground state E_1 and the excited state E_2. Let N_1 and N_2 be the average numbers of atoms in the ground and excited states respectively. The number of states are changed from emission state $E_2 \rightarrow E_1$ with a rate $\frac{dN_{21}}{dt}$, and at any point in time, the number of ground states are determined by absorbed energies from $E_1 \rightarrow E_2$ with a rate $\frac{dN_{12}}{dt}$ respectively. For convenience of description, let N_{12} be the number of atoms from E_1 to E_2 and N_{21} be the numbers from E_2 to E_1. In Einstein's model, a measurement quaternion is $\langle N_1, N_2, N_{12}, N_{21} \rangle$.

2.2.2 Spin measurements

Uhlenback and Goudsmit proposed spin using devices devised by Stern-Gerlach [Cohn (1990); Jammer (1974)]. Spin can be represented by $|\uparrow\rangle, |\downarrow\rangle$ in a two-state system. A quaternion $\langle\langle\uparrow|\uparrow\rangle, \langle\uparrow|\downarrow\rangle, \langle\downarrow|\uparrow\rangle, \langle\downarrow|\downarrow\rangle\rangle$ can be established for spin interactions.

CHSH proposed spin measures testing Bell Inequalities [Aspect (2002); Clauser et al. (1969)]. They applied $\perp \rightarrow +$ and $\| \rightarrow -$ to establish a measurement quaternion:
$\langle N_{++}, N_{+-}, N_{-+}, N_{--} \rangle$. CHSH parameters are in the Stern-Gerlach scheme.

2.2.3 Aspect's measurements

Advanced experimental testing of Bell Inequalities for quantum measures were performed by [Aspect (2002); Aspect et al. (1982)]. In this set of experiments, active properties are measured via four measurements: transmission rate N_t, reflection rate N_r, correspondent rate N_c and also the total number N_ω in ω-time period. This set of measurements is a quaternion $\langle N_t, N_r, N_c, N_\omega \rangle$. Among these, N_c is a new data type not found in the Einstein and Stern-Gerlach schemes. As a matched pair of signals, this parameter indicates either single or double path issues. This parameter could be an extension of synchronous/asynchronous time-measurement.

3. Variant simulation and representation system

A comprehensive process of measurement from local interactions through to global matrix representations is described. It is hoped that this may offer a convenient path to assist theorists and experimenters seeking to devise experiments to further explore such natural mysteries through the application of sound principles of logic and measurement.

Using the variant principle described in the next subsections, a N bit 0-1 vector X and a given logic function f, all N bit vectors are exhausted, variant measures generate two groups of histograms. The variant simulation and representation system is shown in Fig 2 (a-b). The detailed principles and methods are described in Sections 3.2-3.7 respectively.

3.1 Simulation and representation model

The full measurement and representation architecture as shown in Figure 2(a) is composed of four components: Meta Measurements MM, Local Interactive Measurements LIM, Statistical

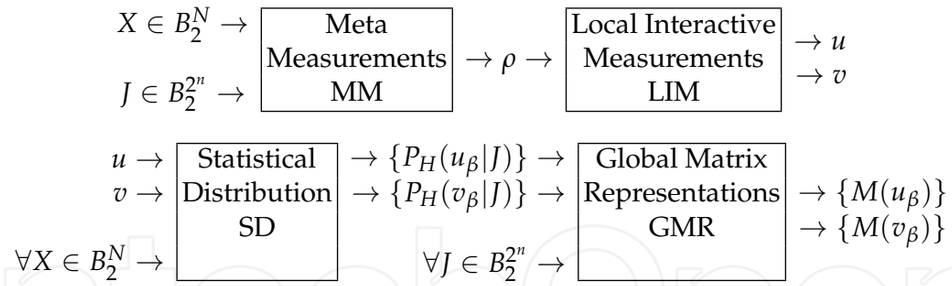

(a) Architecture

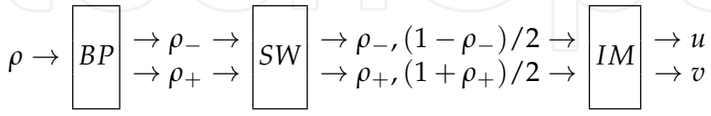

(b) LIM Component

Fig. 2. (a-b) Variant Simulation and Representation System; (a) System Architecture; (b) Local Interactive Measurement LIM Component

Distributions SD, Global Matrix Representations GMR respectively. The key part of the system: the LIM component is shown in Fig 2(b).

3.1.1 Meta Measurements

The Meta Measurement (MM) component uses N bit 0-1 vector X and a given function $J \in B_2^{2^n}$, MM transfers N bit 0-1 vector under $J(X)$ to generate four Meta-measures, under a given Probability scheme, four probability measurements are generated to output as a quaternion signal ρ.

3.1.2 Local Interactive Measurements

The Local Interactive Measurement (LIM) component is the key location for local interactions as shown in Figure 2(b) to transfer quaternion signal ρ under symmetry / anti-symmetry and synchronous / asynchronous conditions, in relation to four combination of time effects as (Left, Right, Double Particle, Double Wave) respectively. Two types of additive operations are identified. Each $\{u, v\}$ signal is composed of four distinct signals.

3.1.3 Statistical Distributions

The Statistical Distribution (SD) component performs statistical activities on corresponding signals. It is necessary to exhaust all possible vectors of X with a total of 2^N vectors. Under this construction, each sub-signal of $\{u, v\}$ forms a special histogram with a one dimensional spectrum to indicate the distribution under function J. A total of eight histograms are generated in the probability conditions.

3.1.4 Global Matrix Representations

The Global Matrix Representation (GMR) component uses each statistical distribution of the relevant probability histogram as an element of a matrix composed of a total of 2^{2^n} elements

for all possible functions $\{J\}$. In this configuration, C code schemes are applied to form a $2^{2^{n-1}} \times 2^{2^{n-1}}$ matrix to show the selected distribution group.

Unlike the other coding schemes (SL, W, F, ...), only C code schemes provide a regular configuration to clearly differentiate the Left path as exhibiting horizontal actions and the Right path as exhibiting vertical actions . Such clearly polarized outcomes may have the potential to help in the understanding of interactive mechanism(s) between double path for particles and double path for waves properties.

3.2 Variant principle

The variant principle is based on n-variable logic functions [Zheng (2011); Zheng & Zheng (2010; 2011a;b); Zheng et al. (2011)].

3.2.1 Two sets of states

For any n-variables $x = x_{n-1}...x_i...x_0$, $0 \leq i < n, x_i \in \{0,1\} = B_2$ let a position j be the selected bit $0 \leq j < n$, x_j be the selected variable. Let output variable y and n-variable function $f, y = f(x)$, $y \in B_2, x \in B_2^n$. For all states of x, a set $S(n)$ composed of the 2^n states can be divided into two sets: $S_0(n)$ and $S_1(n)$.

$$\begin{cases} S_0(n) = \{x | x_j = 0, \forall x \in B_2^n\} \\ S_1(n) = \{x | x_j = 1, \forall x \in B_2^n\} \\ S(n) = \{S_0(n), S_1(n)\} \end{cases} \tag{1}$$

3.2.2 Four meta functions

For a given logic function f, input and output pair relationships define four meta logic functions $\{f_\perp, f_+, f_-, f_\top\}$.

$$\begin{cases} f_\perp(x) = \{f(x) | x \in S_0(n), y = 0\} \\ f_+(x) = \{f(x) | x \in S_0(n), y = 1\} \\ f_-(x) = \{f(x) | x \in S_1(n), y = 0\} \\ f_\top(x) = \{f(x) | x \in S_1(n), y = 1\} \end{cases} \tag{2}$$

3.2.3 Two polarized functions

Considering two standard logic canonical expressions: AND-OR form is selected from $\{f_+(x), f_\top(x)\}$ as $y = 1$ items, and OR-AND form is selected from $\{f_-(x), f_\perp(x)\}$ as $y = 0$ items. Considering $\{f_\top(x), f_\perp(x)\}$, $x_j = y$ items, they are invariant themselves.

To select $\{f_+(x), f_-(x)\}, x_j \neq y$ in forming variant logic expression. Let $f(x) = \langle f_+ | x | f_- \rangle$ be a variant logic expression. Any logic function can be expressed as a variant logic form. In $\langle f_+ | x | f_- \rangle$ structure, f_+ selected 1 items in $S_0(n)$ as same as the AND-OR standard expression, and f_- selecting relevant parts the same as OR-AND expression 0 items in $S_1(n)$.

3.2.4 $n = 2$ representation

For a convenient understanding of the variant representation, 2-variable logic structures are illustrated for its 16 functions as follows.

f	$f\in$	3	2	1	0	$f_+\in$	3^0	2^1	1^0	0^1	$f_-\in$
$No.$	$S(n)$	11	10	01	00	$S_0(n)$	11^0	10^1	01^0	00^1	$S_1(n)$
0	$\{\emptyset\}$	0	0	0	0	$\langle\emptyset\|$	1	0	1	0	$\|3,1\rangle$
1	$\{0\}$	0	0	0	1	$\langle 0\|$	1	0	1	1	$\|3,1\rangle$
2	$\{\emptyset\}$	0	0	1	0	$\langle\emptyset\|$	1	0	0	0	$\|3\rangle$
3	$\{1,0\}$	0	0	1	1	$\langle 0\|$	1	0	0	1	$\|3\rangle$
4	$\{2\}$	0	1	0	0	$\langle 2\|$	1	1	1	0	$\|3,1\rangle$
5	$\{2,0\}$	0	1	0	1	$\langle 2,0\|$	1	1	1	1	$\|3,1\rangle$
6	$\{2,1\}$	0	1	1	0	$\langle 2\|$	1	1	0	0	$\|3\rangle$
7	$\{2,1,0\}$	0	1	1	1	$\langle 2,0\|$	1	1	0	1	$\|3\rangle$
8	$\{3\}$	1	0	0	0	$\langle\emptyset\|$	0	0	1	0	$\|1\rangle$
9	$\{3,0\}$	1	0	0	1	$\langle 0\|$	0	0	1	1	$\|1\rangle$
10	$\{3,1\}$	1	0	1	0	$\langle\emptyset\|$	0	0	0	0	$\|\emptyset\rangle$
11	$\{3,1,0\}$	1	0	1	1	$\langle 0\|$	0	0	0	1	$\|\emptyset\rangle$
12	$\{3,2\}$	1	1	0	0	$\langle 2\|$	0	1	1	0	$\|1\rangle$
13	$\{3,2,0\}$	1	1	0	1	$\langle 2,0\|$	0	1	1	1	$\|1\rangle$
14	$\{3,2,1\}$	1	1	1	0	$\langle 2\|$	0	1	0	0	$\|\emptyset\rangle$
15	$\{3,2,1,0\}$	1	1	1	1	$\langle 2,0\|$	0	1	0	1	$\|\emptyset\rangle$

(3)

Checking two functions $f=3$ and $f=6$ respectively.
$\{f=3:=\langle 0|3\rangle, f_+=11:=\langle 0|\emptyset\rangle, f_-=2:=\langle\emptyset|3\rangle\}$;
$\{f=6:=\langle 2|3\rangle, f_+=14:=\langle 2|\emptyset\rangle, f_-=2:=\langle\emptyset|3\rangle\}$.

3.3 Meta measures

Under variant construction, N bits of 0-1 vector X under a function J produce four Meta measures composed of a measure vector N

$(X:J(X))\to(N_\perp,N_+,N_-,N_\top), N=N_\perp+N_++N_-+N_\top$

Using four Meta measures, relevant probability measurements can be formulated.
$\rho=(\rho_\perp,\rho_+,\rho_-,\rho_\top)=(N_\perp/N,N_+/N,N_-/N,N_\top/N), 0\le\rho_\perp,\rho_+,\rho_-,\rho_\top\le 1.$

From a methodological viewpoint, this set of probability parameters belongs to *multivariate probability measurements*.

3.3.1 Variant measure functions

Let Δ be the variant measure function

$$\begin{aligned}\Delta&=\langle\Delta_\perp,\Delta_+,\Delta_-,\Delta_\top\rangle\\ \Delta J(x)&=\langle\Delta_\perp J(x),\Delta_+J(x),\Delta_-J(x),\Delta_\top J(x)\rangle\\ \Delta_\alpha J(x)&=\begin{cases}1,\ J(x)\in J_\alpha(x),\alpha\in\{\perp,+,-,\top\}\\ 0,\ \text{others}\end{cases}\end{aligned}\tag{4}$$

For any given n-variable state there is one position in $\Delta J(x)$ to be 1 and other 3 positions are 0.

3.3.2 Variant measures on vector

For any N bit 0-1 vector $X, X=X_{N-1}...X_j...X_0, 0\le j<N, X_j\in B_2, X\in B_2^N$ under n-variable function J, n bit 0-1 output vector Y, $Y=J(X)=\langle J_+|X|J_-\rangle$, $Y=Y_{N-1}...Y_j...Y_0, 0\le j<$

$N, Y_j \in B_2, Y \in B_2^N$. For the j-th position $x^j = [...X_j...] \in B_2^n$ to form $Y_j = J(x^j) = \langle J_+|x^j|J_-\rangle$. Let N bit positions be cyclic linked. Variant measures of $J(X)$ can be decomposed

$$\Delta(X:Y) = \Delta J(X) = \sum_{j=0}^{N-1} \Delta J(x^j) = \langle N_\perp, N_+, N_-, N_\top \rangle \tag{5}$$

as a quaternion $\langle N_\perp, N_+, N_-, N_\top \rangle$, $N = N_\perp + N_+ + N_- + N_\top$.

3.3.3 Example

E.g. $N = 12$, given $J, Y = J(X)$.

$$\begin{aligned} X &= 1\ 0\ 1\ 1\ 1\ 0\ 1\ 1\ 1\ 0\ 0\ 1 \\ Y &= 0\ 0\ 1\ 0\ 1\ 0\ 1\ 0\ 1\ 1\ 0\ 0 \\ \Delta(X:Y) &= -\ \perp\ \top\ -\ \top\ \perp\ \top\ -\ \top\ +\ \perp\ - \end{aligned}$$

$\Delta J(X) = \langle N_\perp, N_+, N_-, N_\top \rangle = \langle 3, 1, 4, 4 \rangle, N = 12$.

Input and output pairs are 0-1 variables for only four combinations. For any given function J, the quantitative relationship of $\{\perp, +, -, \top\}$ is directly derived from the input/output sequences. Four meta measures are determined.

3.4 Four meta measurements

Using variant quaternion, local measurements of probability signals are calculated as four meta measurements by following the given equations. For any N bit 0-1 vector X, function J, under Δ measurement: $\Delta J(X) = \langle N_\perp, N_+, N_-, N_\top \rangle$, $N = N_\perp + N_+ + N_- + N_\top$

Signal ρ is defined by

$$\begin{cases} \rho = \frac{\Delta J(X)}{N} = (\rho_\perp, \rho_+, \rho_-, \rho_\top) \\ \rho_\alpha = \frac{N_\alpha}{N}, \alpha \in \{\perp, +, -, \top\} \end{cases} \tag{6}$$

The four meta measurements are core components in the *multivariate probability framework*.

3.5 Local Interactive Measurements

Local Interactive Measurements (LIM) are divided into three stages: BP, SW and SM respectively. The BP stage selects $\{\rho_-, \rho_+\}$ as sub-signals. The SW component extends two signals into four signals with different symmetric properties; The SM component merges different signals to form two sets of eight signals.

Using $\{\rho_+, \rho_-\}$, a pair of signals $\{u, v\}$ are formulated:

$$\begin{cases} u = (u_+, u_-, u_0, u_1) = \{u_\beta\} \\ v = (v_+, v_-, v_0, v_1) = \{v_\beta\} \\ \quad \beta \in \{+, -, 0, 1\} \end{cases} \tag{7}$$

$$\begin{cases} u_+ = \rho_+ \\ u_- = \rho_- \\ u_0 = u_+ \oplus u_- \\ u_1 = u_+ + u_- \\ v_+ = \frac{1+\rho_+}{2} \\ v_- = \frac{1-\rho_-}{2} \\ v_0 = v_+ \oplus v_- \\ v_1 = v_+ + v_- - 0.5 \end{cases} \tag{8}$$

where $0 \leq u_\beta, v_\beta \leq 1, \beta \in \{+, -, 0, 1\}$, $\oplus$: Asynchronous addition, $+$: Synchronous addition.

3.6 Statistical distributions

The SD component provides a statistical means to accumulate all possible vectors of N bits for a selected signal and generate a histogram. Eight signals correspond to eight histograms respectively. Among these, four histograms exhibit properties of symmetry and another four histograms exhibit properties of anti-symmetry.

3.6.1 Statistical histograms

For a function J, all measurement signals are collected and the relevant histogram represents a complete statistical distribution.

Using u and v signals, each u_β or v_β determines a fixed position in the relevant histogram to make vector X on a position. After completing 2^N data sequences, eight symmetry/anti-symmetry histograms of $\{H(u_\beta|J)\}, \{H(v_\beta|J)\}$ are generated.

For a function J, $\beta \in \{+, -, 0, 1\}$

$$\begin{cases} H(u_\beta|J) = \sum_{\forall X \in B_2^N} H(u_\beta|J(X)) \\ H(v_\beta|J) = \sum_{\forall X \in B_2^N} H(v_\beta|J(X)), J \in B_2^{2^n} \end{cases} \tag{9}$$

3.6.2 Probability histograms

Let $|H(..)|$ denote the total number in the histogram $H(..)$, a normalized Probability histogram ($P_H(..)$) can be expressed as

$$\begin{cases} P_H(u_\beta|J) = \frac{H(u_\beta|J)}{|H(u_\beta|J)|} \\ P_H(v_\beta|J) = \frac{H(v_\beta|J)}{|H(v_\beta|J)|}, J \in B_2^{2^n} \end{cases} \tag{10}$$

Here, all histograms are restricted in $[0, 1]^2$ areas respectively.

Distributions are dependant on the data set as a whole and are not sensitive to varying under special sequences. Under this condition, when the data set has been exhaustively listed, then the same distributions are always linked to the given signal set.

The eight histogram distributions provide invariant spectrum to represent properties among different interactive conditions.

3.7 Global Matrix Representations

After local interactive measurements and statistical process are undertaken for a given function J, eight histograms are generated. The Global Matrix Representation GMR component performs its operations into two stages. In the first stage, exhausting all possible functions for $\forall J \in B_2^{2^n}$ to generate eight sets, each set contains 2^{2^n} elements and each element is a histogram. In the second stage, arranging all 2^{2^n} elements generated as a matrix by C code scheme. Here, we can see Left and Right path reactions polarized into Horizontal and Vertical relationships respectively.

3.7.1 Matrix and Its elements

For a given C scheme, let $C(J) = \langle J^1|J^0\rangle$, each element

$$\begin{cases} M_{\langle J^1|J^0\rangle}(u_\beta|J) = P_H(u_\beta|J) \\ M_{\langle J^1|J^0\rangle}(v_\beta|J) = P_H(v_\beta|J) \\ \qquad J \in B_2^{2^n};\ J^1, J^0 \in B_2^{2^{n-1}} \end{cases} \tag{11}$$

3.7.2 Representation patterns of matrices

For example, using $n = 2, P = (3102), \Delta = (1111)$ conditions, a C code case contains sixteen histograms arranged as a 4×4 matrix.

0	4	1	5
2	6	3	7
8	12	9	13
10	14	11	15

(12)

All matrices in this chapter use this configuration for the matrix pattern to represent their elements.

4. Simulation results

For ease of illustration, as different signals have intrinsic random properties only statistical distributions and global matrix representations are selected in this section.

4.1 Statistical distributions

The simulation provides a series of output results. In this section, $N = \{12, 13\}, n = 2, \{J = 3, J_+ = 11, J_- = 2\}$ are selected. Corresponding to Left path (Left), Right path (Right), Double path for Particles (D-P) and Double path for Waves (D-W) under symmetry and anti-symmetry conditions respectively.

From a given function, a set of histograms can be generated as two groups of eight probability histograms. To show their refined properties, it is necessary to represent them in both odd and even numbers. A total of sixteen histograms are required. For convenience of comparison, sample cases are shown in Figures 3(I-III).

$P_H(u_+\|J)$	$P_H(u_-\|J)$
(a) Left	(b) Right
$P_H(u_0\|J)$	$P_H(u_1\|J)$
(c) D-P	(d) D-W
$P_H(v_+\|J)$	$P_H(v_-\|J)$
(e) Left	(f) Right
$P_H(v_0\|J)$	$P_H(v_1\|J)$
(g) D-P	(h) D-W

(I) Representative patterns of Histograms for function J (a-d) symmetric cases; (e-h) antisymmetric cases

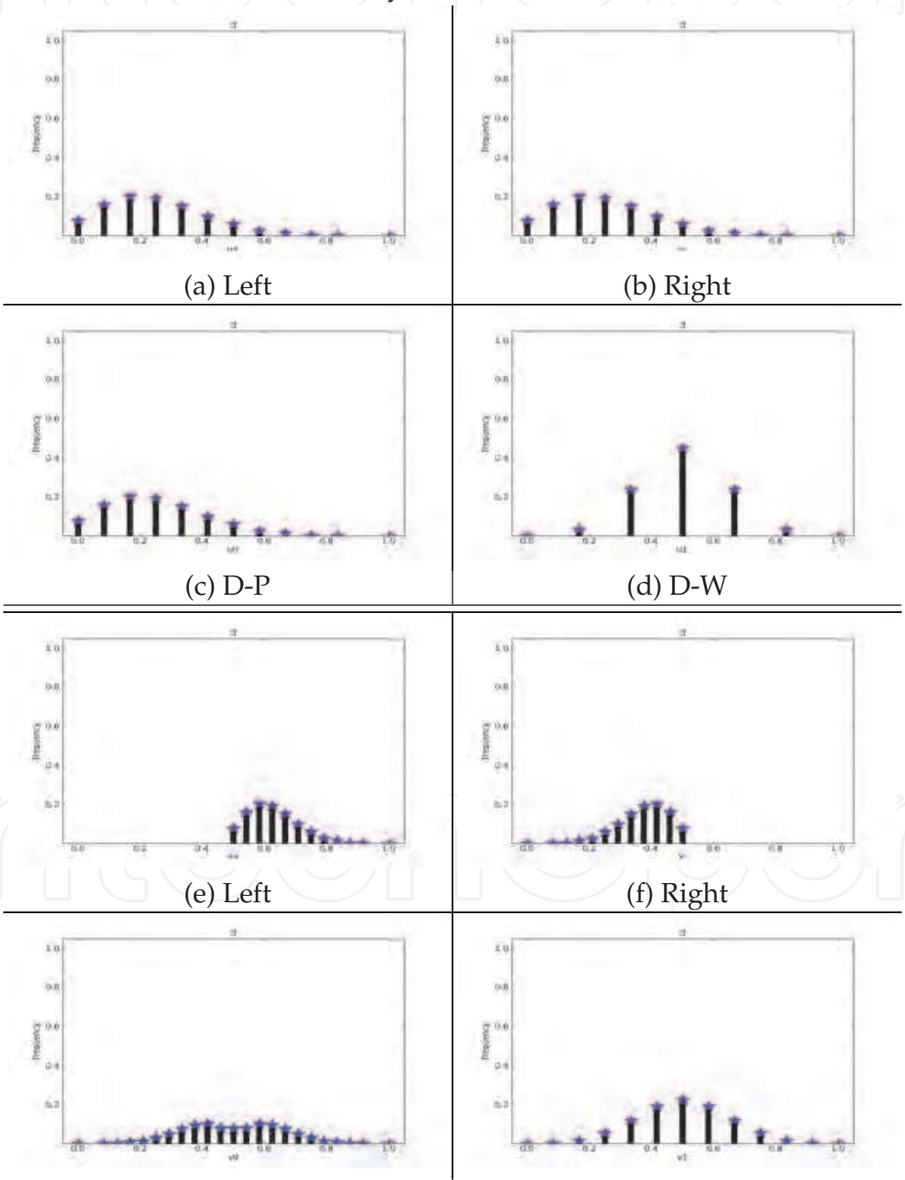

(a) Left (b) Right

(c) D-P (d) D-W

(e) Left (f) Right

(g) D-P (h) D-W

(II) $N = \{12\}$, $J = 3$ Two groups of results in eight histograms

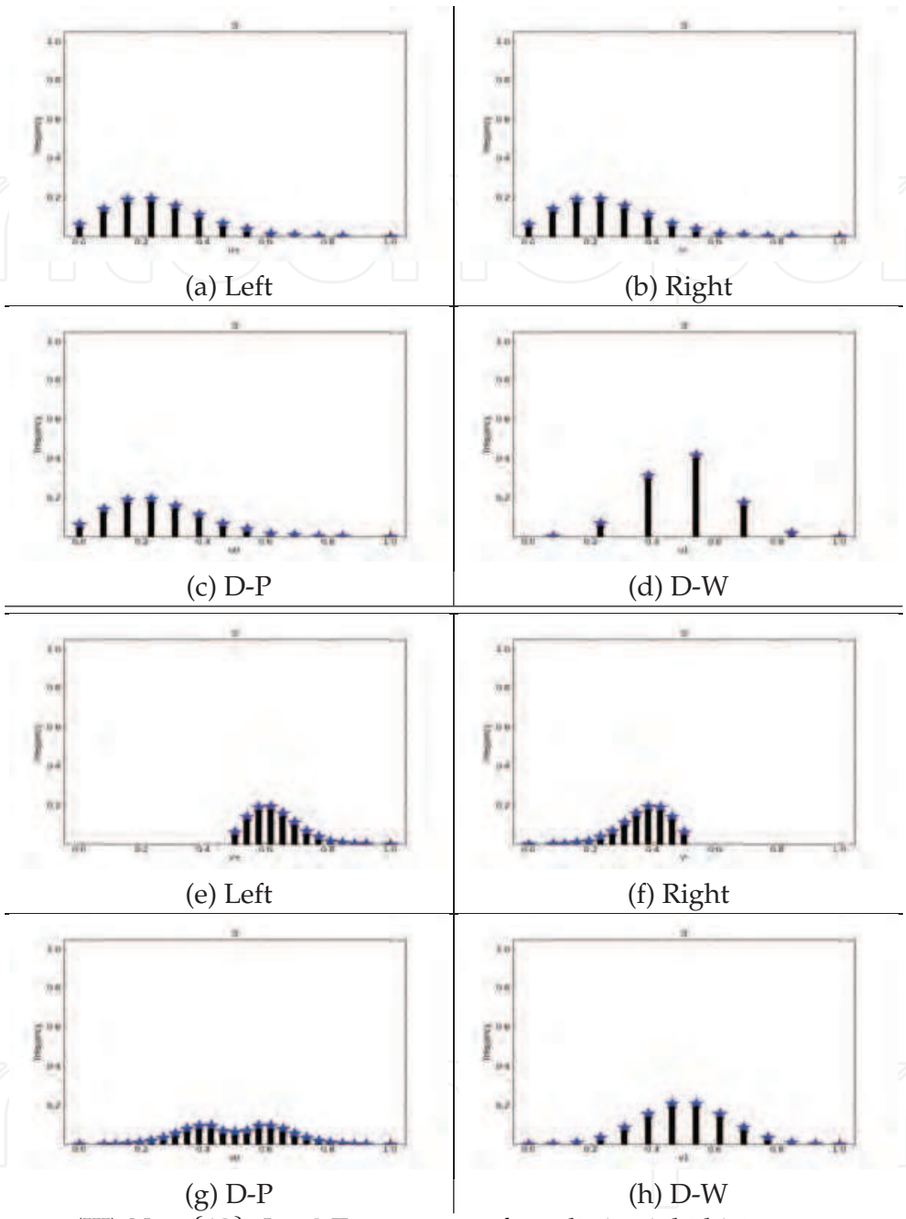

(a) Left (b) Right

(c) D-P (d) D-W

(e) Left (f) Right

(g) D-P (h) D-W

(III) $N = \{13\}, J = 3$ Two groups of results in eight histograms

Fig. 3. (I-III) $N = \{12, 13\}, J = 3$ Simulation results ; (I) Representative Patterns for $P_H(u_+|J) = P_H(u_-|J)$ and $P_H(v_+|J) = P_H(1 - v_-|J)$ conditions; (II) $N = \{12\}, J = 3$ Two groups of eight probability histograms; (III) $N = \{13\}, J = 3$ Two groups of eight probability histograms

Representation patterns are illustrated in Fig 3(I). Eight probability histograms of $P_H(u_+|J) = P_H(u_+|J)$ are shown in Fig 3(II) for $N = 12$ to represent four symmetry groups and another eight probability histograms are shown Fig 3(III) for $N = 13$ to represent four anti-symmetry groups respectively.

4.2 Global matrix representations

All possible 2^{2^n} functions are applied. It is convenient to arrange all generated histograms as a matrix, a C code scheme of variant logic applied to organize a set of 2^{2^n} histograms into a $2^{2^{n-1}} \times 2^{2^{n-1}}$ matrix.

Applying the C code configuration, a given signal of a function determines an element on a matrix to represent its histogram. There is one to one correspondence among different configurations.

Using this measurement mechanism, eight types of statistical histograms are systematically illustrated. Each element in the matrix is numbered to indicate its corresponding function and also the relevant histogram will be put on the position.

For $n = 2$ cases, sixteen matrices are shown in Figs 5-6 (a-h). Figs 5-6 (a-d) represent Symmetry groups and Figs 5-6 (e-h) represent Anti-symmetry groups. To show odd and even number configurations, Fig 5 (a-h) shows $N = 12$ cases and Fig 6 (a-h) shows $N = 13$ cases respectively.

5. Analysis of results

In the previous section, results of different statistical distributions and their global matrix representations were presented. In this section, plain language is used to explain what various visual effects might be illustrated and to discuss local and global arrangements.

5.1 Statistical distributions for a given function

It is essential to analyze differences among various statistical distributions for a given function.

5.1.1 Symmetry groups for a function

For the selected function $J = 3$, four distributions in symmetry groups are shown in Fig 3 (a-d). (a) $P_H(u_+|J)$ for Left; (b) $P_H(u_-|J)$ for Right; (c) $P_H(u_0|J)$ for D-P; and (d) $P_H(u_1|J)$ for D-W respectively.

Under Symmetry conditions, $P_H(u_+|J) = P_H(u_-|J)$, both Left and Right distributions are the same. $P_H(u_0|J)$ generated with both paths open under asynchronous conditions simulates D-P. Compared with distributions in (a-b) , it is feasible to identify the same components from original inputs.

However, for $P_H(u_1|J)$ under synchronous conditions and with the same Left and Right input signals, the simulation shows D-W exhibiting interferences among the output distributions that are significantly different from the original components.

5.1.2 Anti-symmetry groups for a function

Four distributions are shown in Fig 3 (e-h) as asymmetry groups. A pair of equation $P_H(v_+|J) = P_H(1 - v_-|J)$ shows that one distribution is a mirror image of another one. $P_H(v_+|J)$ distribution is shown in Fig 3 (e) for Left signals and $P_H(v_-|J)$ distribution is shown Fig 3 (f) for Right signals.

$P_H(v_0|J)$ is shown in Fig 3 (g) for both paths open under asynchronous conditions to simulate D-P. Compared with (e-f) distributions, it is feasible to identify the same components from the original inputs.

However $P_H(v_1|J)$ is shown in Fig 3 (h) under synchronous condition with both path signals as inputs to simulate D-W exhibiting interferences among the output distributions that are significantly different from the original components.

To show even and odd number's differences, $N = 12$ cases are shown in Fig 3 (II, a-h) and $N = 13$ cases are shown in Fig 3 (III, a-h) respectively.

5.2 Global matrix representations

Sixteen matrices are represented in Fig 4-5 (a-h) with eight signals generating two sets of 16 groups for $N = \{12, 13\}$ respectively.

5.2.1 Symmetry cases

Matrices for the Left in Fig 4-5 (a) show elements in a column with the corresponding histogram showing polarized effects on the vertical.

Matrices for the Right in Fig 4-5 (b) show elements in a row with the corresponding histogram showing polarized effects on the horizontal.

Matrices for D-P in Fig 4-5 (c) provide asynchronous operations combined with both distributions from Fig 4-5 (a-b) to form a unified distribution. From each corresponding position, it is possible to identify each left and right component and the resulting shapes of the histogram.

Matrices for D-W in Fig 4-5 (d) provide synchronous operations combined with both distributions from Fig 4-5 (a-b) for each element. Compared with Fig 4-5 (c) and Fig 4-5 (d) respectively, distributions in Fig 4-5 (d) are much simpler with two original distributions especially on the anti-diagonal positions: $J \in \{10, 12, 3, 5\}$. Only less than half the number of spectrum lines are identified.

5.2.2 Anti-symmetry cases

In a similar manner to the symmetry conditions, four anti-symmetry effects can be identified in Fig 4-5 (e-h). Matrices in Fig 4-5 (e) are Left operations for different functions, elements are polarized on the vertical and matrices in Fig 4-5 (f) are Right operations, elements are polarized on the horizontal. Spectrum lines in Fig 4-5 (e) appear in the right half and spectrum lines in Fig 4-5 (f) are appeared in the left half respectively.

Matrices for D-P in Fig 4-5 (g) show additional effects for each distribution according to the relevant position with components that can be identified as corresponding to identifiable inputs in many cases. Anti-symmetry signals are generated in merging conditions.

Matrices for D-W in Fig 4-5 (h) show different properties. In general, only one peak can be observed for each element especially for the $J \in \{10, 12, 3, 5\}$ condition. Spectra appear to be much simpler than the original distributions in Fig 4-5 (e-f), and significant interference properties are observed.

5.3 Four symmetry groups

Pairs of relationships can be checked on symmetry matrices in Figs 4-5 (a-d), four groups are identified.

5.3.1 Left: polarized vertical group

$\{P_H(u_+|J)\}$ elements in Figs 4-5 (a) show (only) four distinct distributions. Each column contains only one distribution. Sixteen elements in the matrix can be classified into four vertical classes: $\{0, 2, 8, 10\}, \{4, 6, 12, 14\}, \{1, 3, 9, 11\}, \{5, 7, 13, 15\}$ respectively. Four meta distributions are given as $\{10, 14, 11, 15\}$.

5.3.2 Right: polarized horizontal group

$\{P_H(u_-|J)\}$ elements in Figs 4-5 (b) show (a further) four distinct distributions. Each row contains only one distribution. Sixteen elements in the matrix can be classified into four horizontal classes: $\{0, 4, 1, 5\}, \{2, 6, 3, 7\}, \{8, 12, 9, 13\}, \{10, 14, 11, 15\}$ respectively. Four meta distributions are given as $\{0, 2, 8, 10\}$.

5.3.3 D-P: particle group

$\{P_H(u_0|J)\}$ elements in Figs 4-5 (c) illustrate symmetry properties. There are six pairs of symmetry elements: $\{8 : 14\}, \{2 : 11\}, \{0 : 15\}, \{6 : 9\}, \{4 : 13\}, \{1 : 7\}$. In addition, four elements on anti-diagonals provide different distributions: $\{10, 12, 3, 5\}$. Under this condition, ten classes of distributions are distinguished.

5.3.4 D-W: wave group

$\{P_H(u_1|J)\}$ elements in Figs 4-5 (d) illustrate symmetry properties. There are six pairs of symmetry elements: $\{8 : 14\}, \{2 : 11\}, \{0 : 15\}, \{6 : 9\}, \{4 : 13\}, \{1 : 7\}$. In addition, four elements on diagonal positions provide same distribution: $\{0, 6, 9, 15\}$. Two elements on anti-diagonals: $\{12, 3\}$ have the same distribution in Fig 4 (d). Under this condition, nine or ten classes of different distributions can be identified for Fig 4 (d) and Fig 5 (d) respectively.

5.4 Four anti-symmetry groups

Figures 4-5 (e-h) represent anti-symmetry properties, four groups can be identified.

5.4.1 Left: polarized vertical group

$\{P_H(v_+|J)\}$ elements in Figs 4-5 (e) show that (only) four classes can be distinguished. Elements within these groups members are the same as for symmetry groups in Figs 4-5(a). Their distributions fall within the region $[0.5, 1]$.

5.4.2 Right: polarized horizontal group

$\{P_H(v_-|J)\}$ elements in Figs 4-5 (f) show that (only) four classes can be distinguished. Elements within these groups are the same as for symmetry groups in Figs 4-5 (b). Their distributions fall within the region $[0, 0.5]$.

5.4.3 D-P: particle group

$\{P_H(v_0|J)\}$ in Figs 4-5 (g) show six pairs of anti-symmetry distributions: $\{8 \nmid 14\}, \{2 \nmid 11\}, \{0 \nmid 15\}, \{6 \nmid 9\}, \{4 \nmid 13\}, \{1 \nmid 7\}$ four elements are distinguished on the anti-diagonals: $\{10, 12, 3, 5\}$. Under this condition, ten classes can be identified.

5.4.4 D-W: wave group

$\{P_H(v_1|J)\}$ in Figs 4-5 (h) show six pairs of anti-symmetry distributions: $\{8 \nmid 14\}, \{2 \nmid 11\}, \{0 \nmid 15\}, \{6 \nmid 9\}, \{4 \nmid 13\}, \{1 \nmid 7\}$ four pairs of symmetry elements: $\{3 : 5\}, \{10 : 12\}, \{2 : 4\}, \{11 : 13\}$ are distinguished. Under this condition, twelve classes can be identified.

5.5 Odd and even numbers

From a group view point, only D-P and D-W need to be reviewed as different groups in symmetry conditions. Anti-symmetry conditions are unremarkable.

It is reasonable to suggest that anti-symmetry operations will be much easier to distinguish under experimental conditions, since sixteen groups in D-P conditions and twelve groups in D-W conditions will have significant differences. However, under the symmetry conditions (only) minor differences can be identified.

5.5.1 Single and double peaks

Single and Double peaks can be observed in Fig 4(5) (h): $\{3, 5\}$ for even and odd numbers respectively.

For two other members $\{10, 12\}$, (only) single pulse distributions are observed in Figs 4-5 (h) to show the strongest interference results.

5.6 Class numbers in different conditions

To summarize over the different classes, 16 matrices are shown in different numbers of identified classes as follows:

Class No.	Left	Right	D-P	D-W
SE	4	4	10	9
SO	4	4	10	10
AE	4	4	16	12
AO	4	4	16	12

where Left:Left Path, Right: Right Path, D-P: Double Path for Particles, D-W: Double Path for Waves; SE: Symmetry for Even number, SO: Symmetry for Odd number, AE: Anti-symmetry for Even number, AO: Anti-symmetry for Odd number.

5.7 Polarized effects and double path results

In order to contrast the different polarized conditions, it is convenient to compare distributions $\{P_H(u_+|J), P_H(u_-|J\}$ and $\{P_H(v_+|J), P_H(v_-|J\}$ arranged according to the corresponding polarized vertical and horizontal effects. This visual effect is similar to what might be found when using polarized filters in order to separate complex signals into two channels. Different distributions can be observed under synchronous and asynchronous conditions.

5.7.1 Particle distributions and representations

For all symmetry or non-symmetry cases under $\oplus$ asynchronous addition operations, relevant values meet $0 \leq u_0, v_0, u_-, v_-, u_+, v_+ \leq 1$. Checking $\{P_H(u_0|J), P_H(v_0|J)\}$ series, $\{P_H(u_+|J), P_H(u_-|J)\}$ and $\{P_H(v_+|J), P_H(v_-|J)\}$ satisfy following equation.

$$\begin{cases} P_H(u_0|J) = \frac{P_H(u_-|J)+P_H(u_+|J)}{2} \\ P_H(v_0|J) = \frac{P_H(v_-|J)+P_H(v_+|J)}{2} \end{cases} \tag{13}$$

The equation is true for different values of N and n.

5.7.2 Wave distributions and representations

Interference properties are observed in $\{P_H(u_+|J) = P_H(u_-|J)\}$ conditions. Under $+$ synchronous addition operations, relevant values meet $0 \leq u_1, v_1, u_-, v_-, u_+, v_+ \leq 1$. Checking $\{P_H(u_1|J), P_H(v_1|J)\}$ distributions and compared with $\{P_H(u_+|J), P_H(u_-|J)\}$ and $\{P_H(v_+|J), P_H(v_-|J)\}$, non-equations and equations are formulated as follows:

$$\begin{cases} P_H(u_1|J) \neq P_H(u_0|J) \\ P_H(v_1|J) \neq P_H(v_0|J) \end{cases} \tag{14}$$

Spectra in different cases illustrate wave interference properties. Single and double peaks are shown in interference patterns similar to interference effects in classical double slit experiments.

5.7.3 Non-symmetry and non-anti-symmetry

However, for the $\{P_H(u_+|J) \neq P_H(u_-|J)\}$ non-symmetry cases, there are significant differences between $\{P_H(u_0|J), P_H(v_0|J)\}$ and $\{P_H(u_1|J), P_H(v_1|J)\}$. Such cases have interference patterns with more symmetric properties than single path and particle distributions.

Four anti-diagonal positions are linked to symmetry and anti-symmetry pairs, twelve other pairs of functions belong to non-symmetry and non-anti-symmetry conditions. Their meta elements can be identified by the relevant variant expressions.

6. Other relevant measurements and properties

6.1 Quaternion measurements

It is interesting to note the relationship between the variant quaternion and other quaternion measurements.

6.1.1 Variant quaternion

In the variant quaternion, $\Delta f(X) = (N_\perp, N_+, N_-, N_\top)$, $N = N_\perp + N_+ + N_- + N_\top$.

6.1.2 Einstein quaternion

Einstein's two-state system of interaction $(N_1, N_2, N_{12}, N_{21})$ allows the following equations to be established.

$$\begin{cases} N_1 = N_\perp + N_+ \\ N_2 = N_- + N_\top \\ N_{12} = N_+ \\ N_{21} = N_- \\ N = N_1 + N_2 \end{cases} \tag{15}$$

From the equations, the measured pair $\{N_{21}, N_{12}\}$ has a 1-1 correspondence to $\{N_-, N_+\}$.

6.1.3 CHSH quaternion

Selecting $+ \to 1, - \to 0$, CHSH's $N_{\pm,\pm}(a, b)$ measurements meet

$$\begin{cases} N_{+,+}(a,b) \to N_\top \\ N_{+,-}(a,b) \to N_- \\ N_{-,+}(a,b) \to N_+ \\ N_{-,-}(a,b) \to N_\perp \end{cases} \tag{16}$$

$(N_{++}, N_{+-}, N_{-+}, N_{--}) \to (N_\top, N_-, N_+, N_\perp)$, let $N = N_{++} + N_{+-} + N_{-+} + N_{--}$. CHSH quaternion is a permutation of the variant quaternion.

6.1.4 Aspect quaternion

Aspect's quaternion $(N_t, N_r, N_c, N_\omega)$ have following corresponding:

$$\begin{cases} N_t \to N_- \\ N_r \to N_+ \\ N_\omega \to N \end{cases} \tag{17}$$

For N_c, there is no parameter in the variant quaternion for parameter N_c. N_c indicates joined action numbers to distinguish single and double paths, corresponding to $\{u_1, v_1\}$ times.

This parameter is of significance in an actual experiment. In a simulated system, the parameter provides a control coefficient that separates two types of paths $\{u_0, v_0\}$ and $\{u_1, v_1\}$ that would be measured in real experiments.

6.2 Different particle models

From Newton's particles to Young's Double slit experiments, the question of how to distinguish particle and wave measurements has a long history [Hawking & Mlodinow (2010); Penrose (2004)]. From a measurement viewpoint, recent activities testing Bell Inequations can be seen to be consistent with historical viewpoints [Jammer (1974)].

The fundamental assumptions of Bell Inequations are based on a local realism [Eberhard (1978); Fine (1999)]. A key condition of measure theory can be seen in a review of authoritative definitions of local realism [SEP (2009)].

6.2.1 Independent conditions in probability

Kolmogorov developed modern probability construction [Ash & Doléans-Dade (2000)] to use measure theory approaches to handle probability measurements. Modern expressions of Bell Inequalities have many forms [SEP (2009)], all of these are based on the conceptual framework of locality which is understood as the conjunction of independent conditions on probability measurements.

For any independent events A, B,

$$\begin{array}{l} P(A \cap B) = P(A)P(B) \\ P(A \cup B) = P(A) + P(B) - P(A \cap B), 0 \leq P(A), P(B) \leq 1 \\ P(A \cup B) \leq P(A) + P(B) \end{array} \tag{18}$$

Probability measurement expressions play the core role in Bell Inequalities. In real single photon experiments, people found that $P(A \cup B) \leq P(A) + P(B)$ did not hold true.

In quantum reality environment, testing measurements could be $\tilde{P}(A \cup B) > \tilde{P}(A) + \tilde{P}(B)$ under specific conditions.

6.2.2 Bell inequalities and Newton-Einstein-Feynman particle distributions

From a measurement viewpoint, measurements of local realism correspond to a real number construction that links to Kolmogorov probability [Ash & Doléans-Dade (2000)]. von Neumann (1932,1996)'s mathematical foundation of quantum mechanics is based on a complex number construction. By their nature, these measurement constructions reveal significant differences between the classical and complex probability framework.

Probability deductions under local realism must be restricted to real number systems. Under the independent condition, $P(A \cup B) \leq P(A) + P(B)$ is always true.

6.3 Further predictions

Observing modern experiments to test Bell Inequations, it is necessary to measure the events in synchronous conditions to create multiple pairs of photons. Different time conditions indicate asynchronous and synchronous conditions playing a critical role in distinguishing between classical and quantum activities. Experimental evidence and case study results are not sufficient at this time to permit firm propositions. However, a summary of predictions for the measurement construction of variant frameworks which can be extrapolated from the simulations is provided below.

Prediction 1: Left distributions have relationships showing polarized vertical behaviors.

Prediction 2: Right distributions have relationships showing polarized horizontal behaviors.

Prediction 3: D-P distributions have relationships showing classical particle statistical behaviors.

Prediction 4: D-W distributions have relationships showing wave interference statistical behaviors.

Prediction 5: Under the same conditions of Bell Inequations, it will be possible to design and implement experiments to distinguish D-P and D-W distributions in real photon experimental environments.

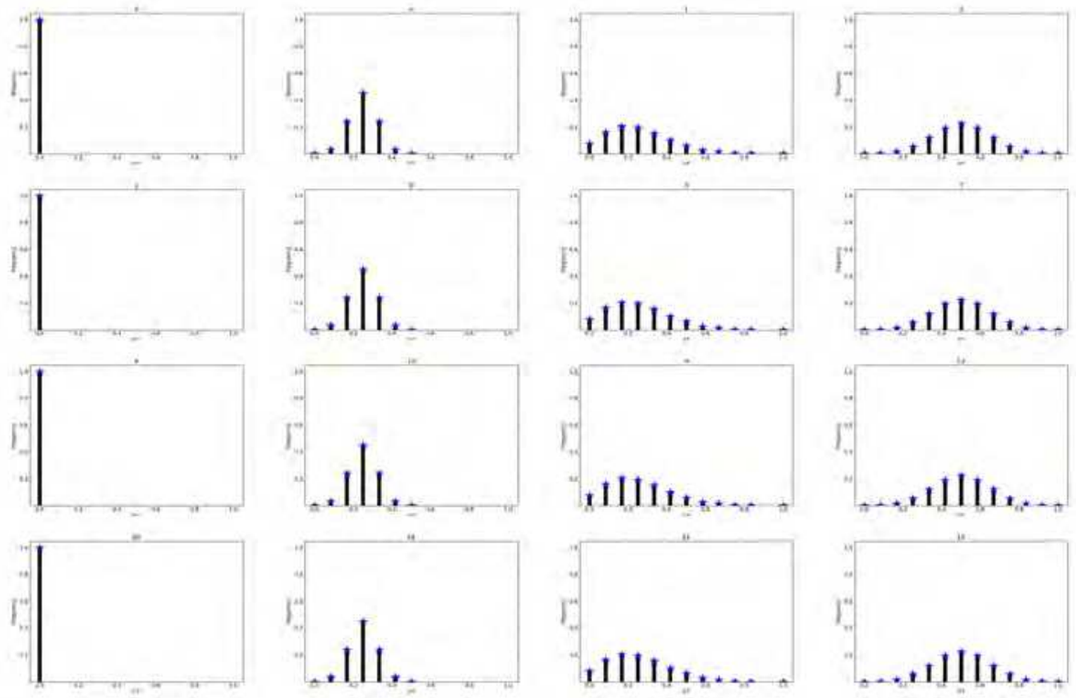

(a) Left

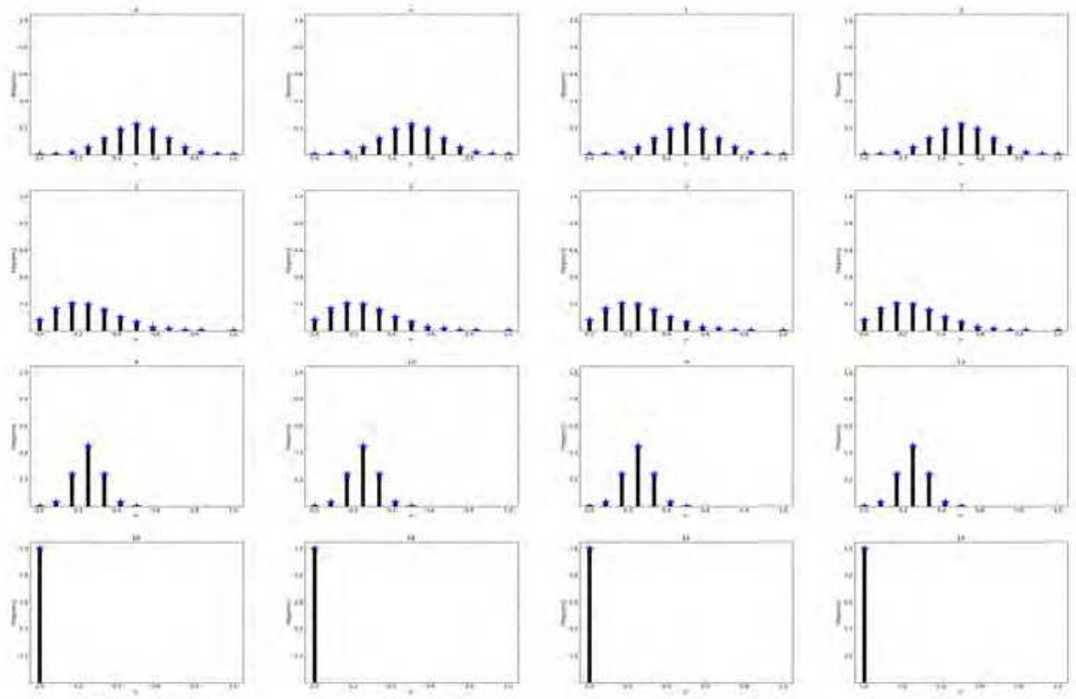

(b) Right

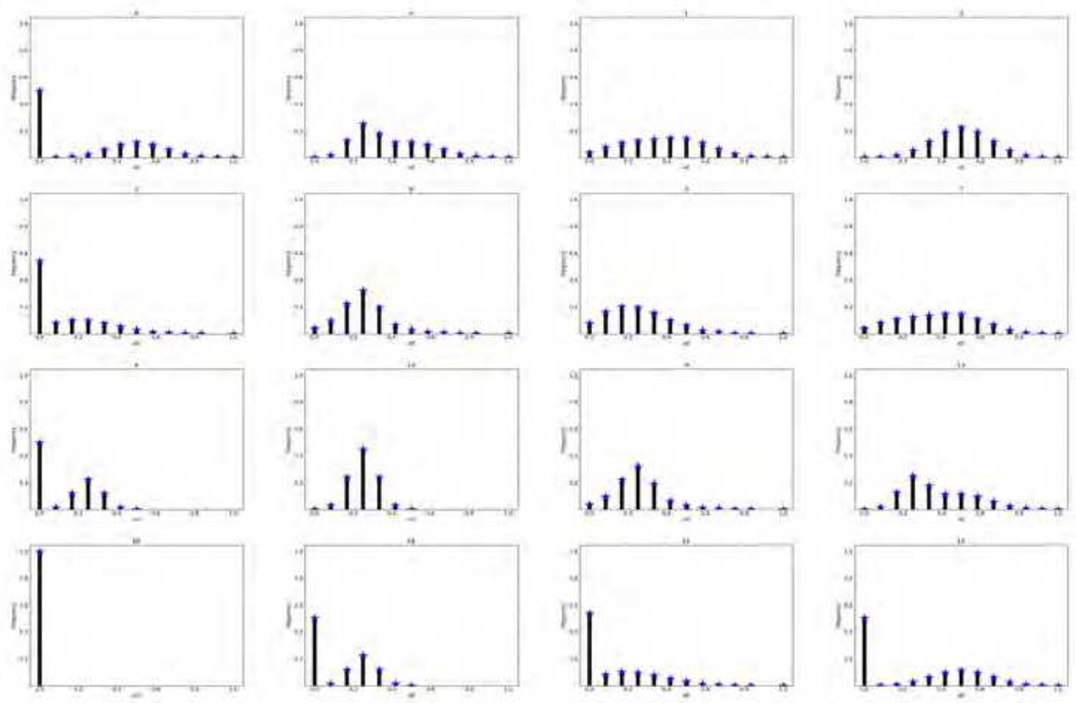

(c) D-P

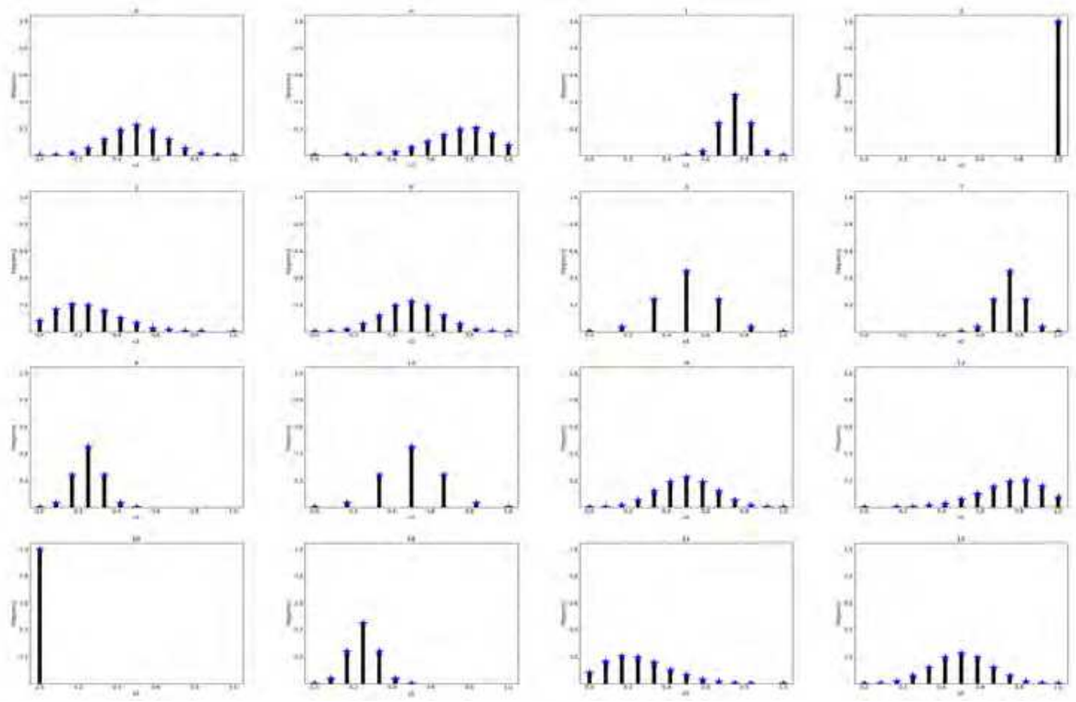

(d) D-W

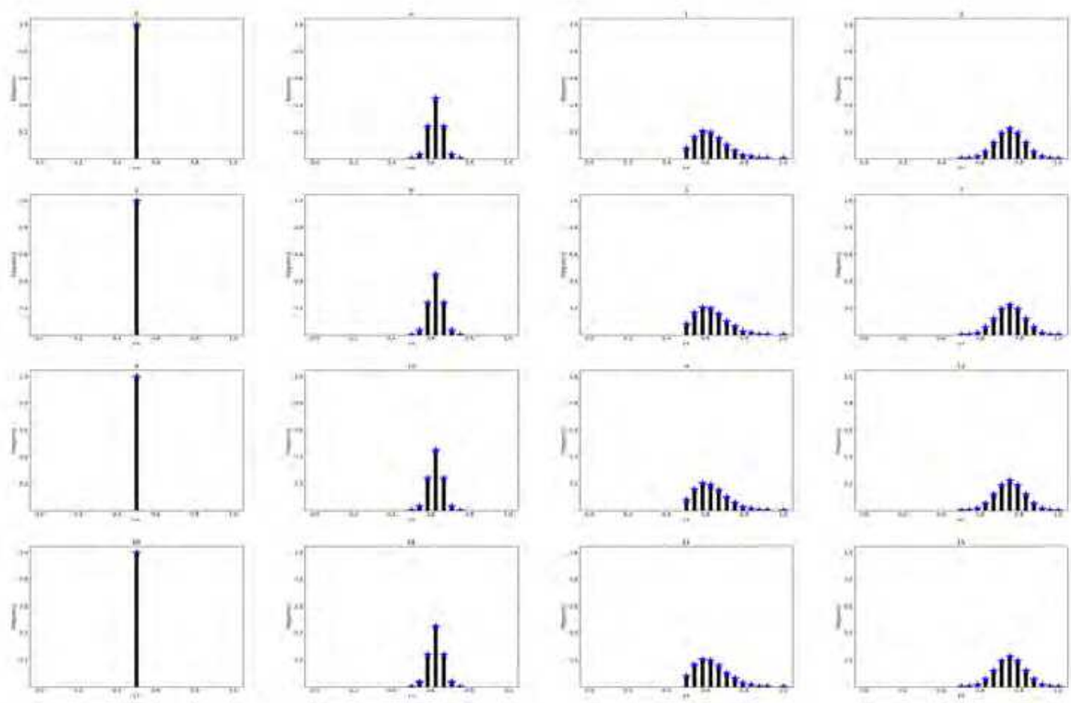

(e) Left

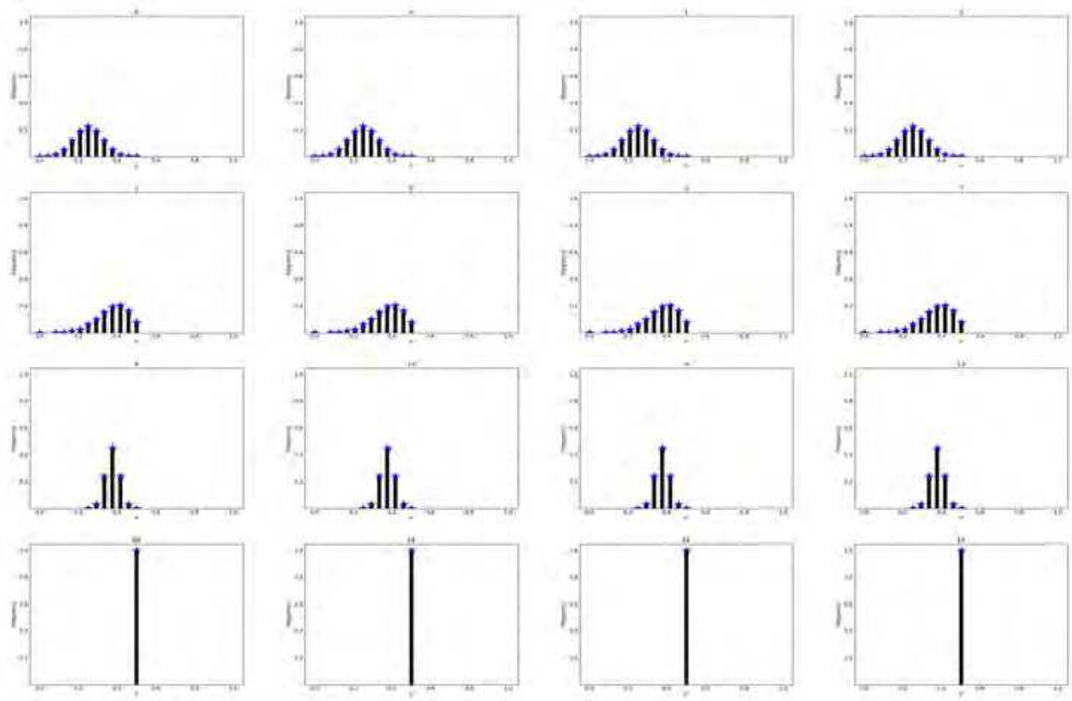

(f) Right

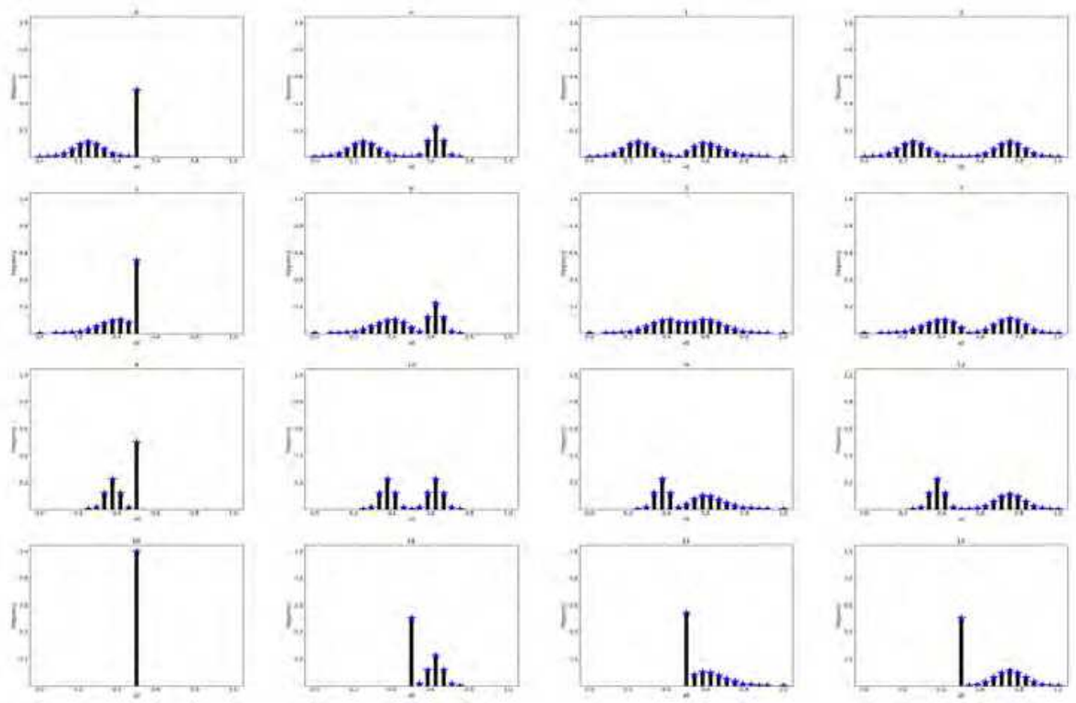

(g) D-P

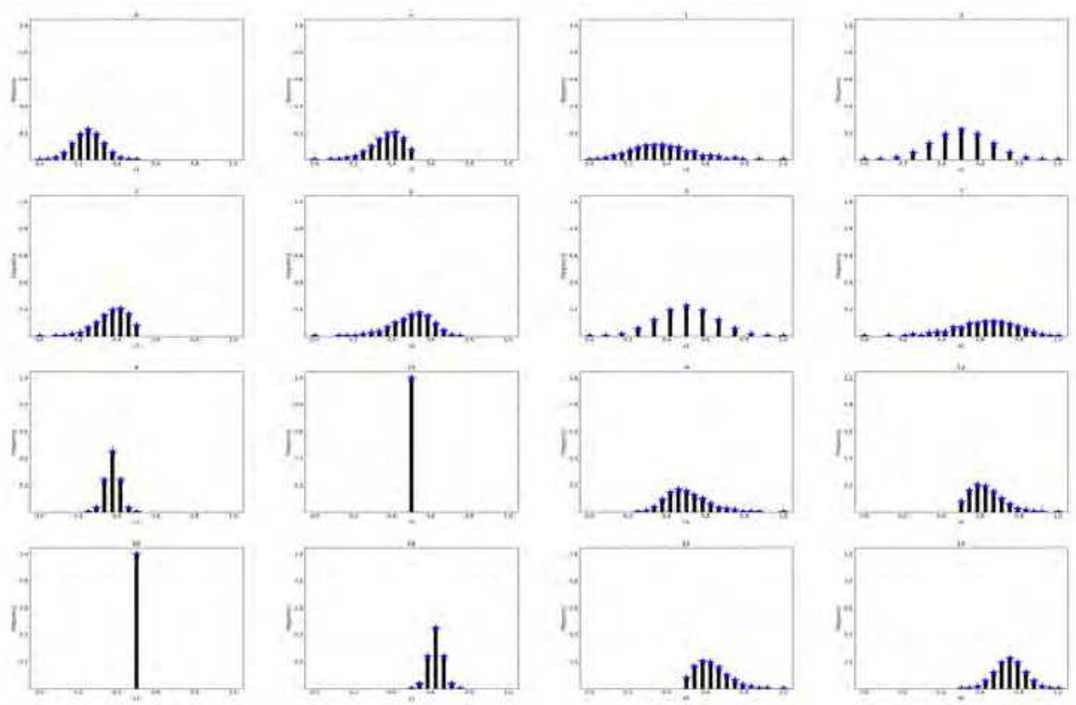

(h) D-W

Fig. 4. (a-h) Even number groups: $N = \{12\}, f \in B_2^4$ Eight Matrices of Global Matrix Representations. (a) Left; (b) Right; (c) D-P; (d)D-W in symmetry conditions; (e) Left; (f) Right; (g) D-P; (h)D-W in anti-symmetry conditions.

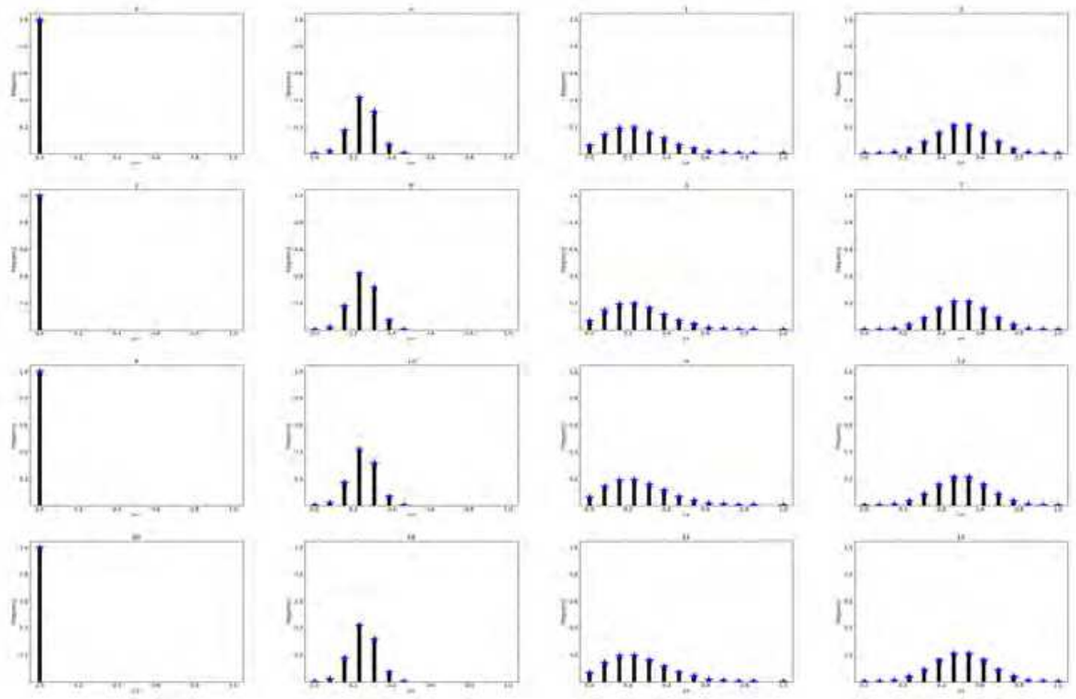

(a) Left

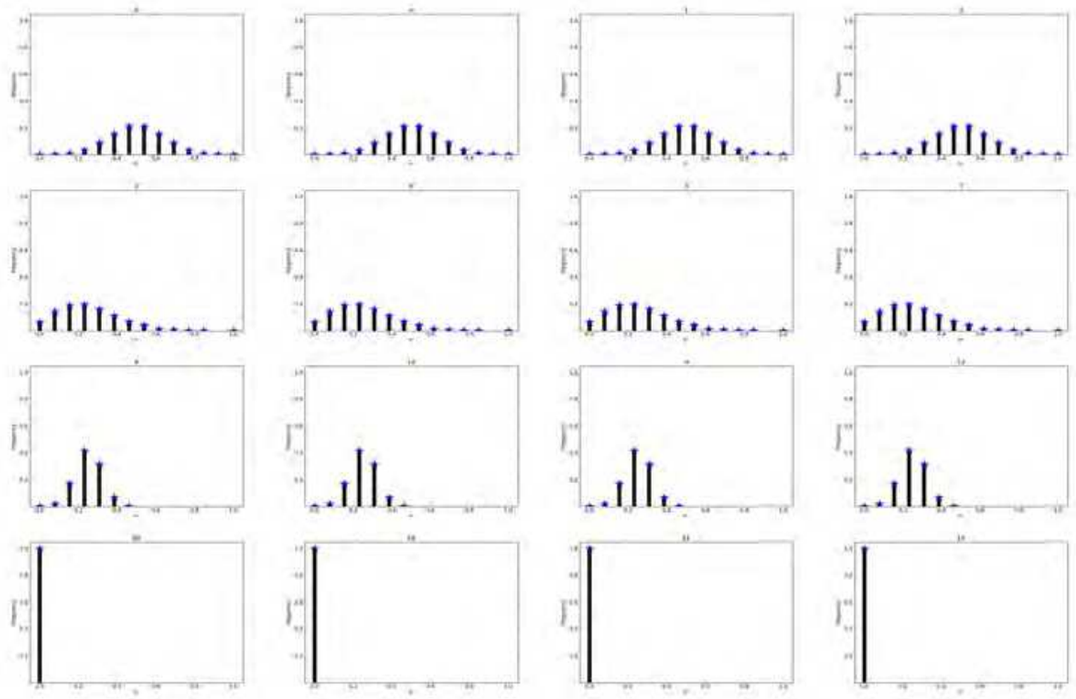

(b) Right

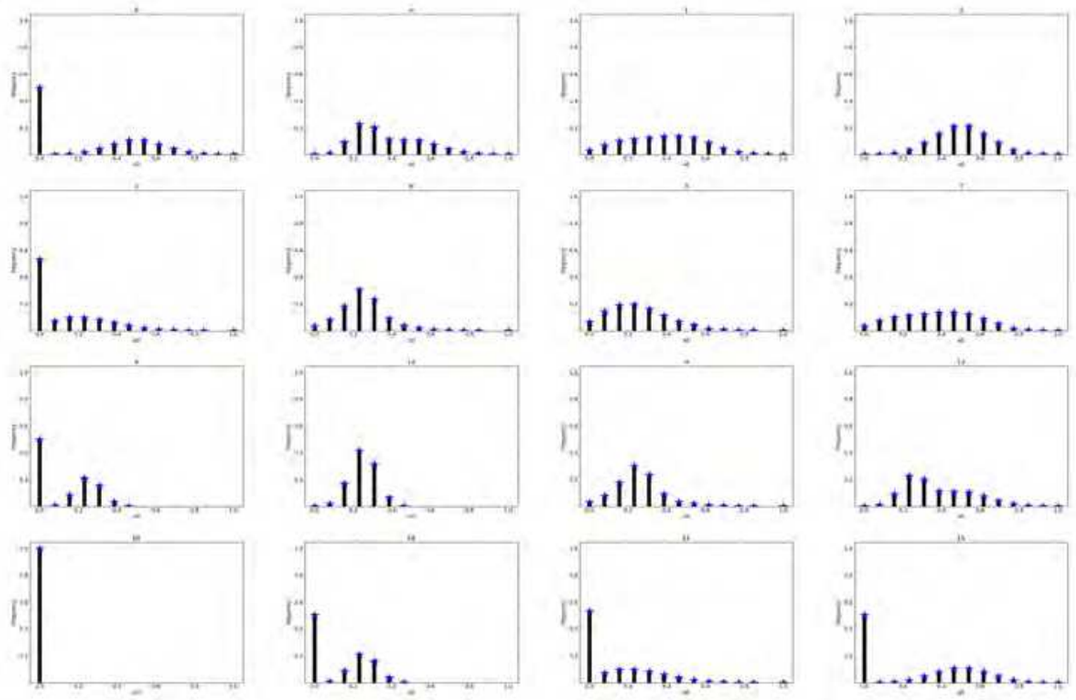

(c) D-P

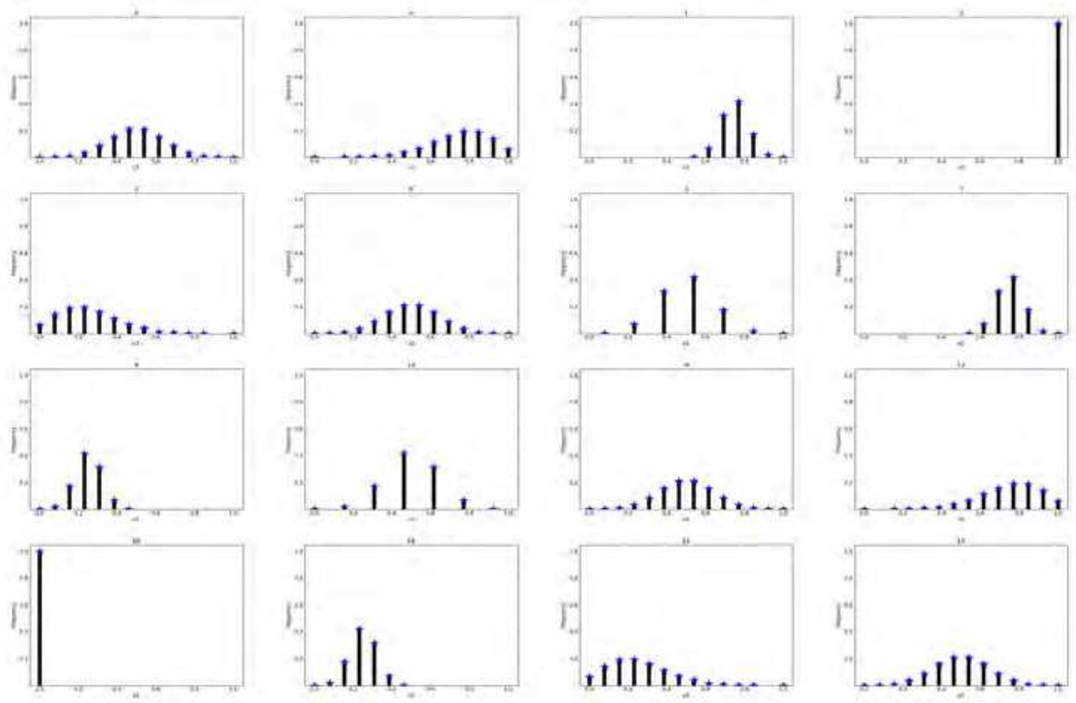

(d) D-W

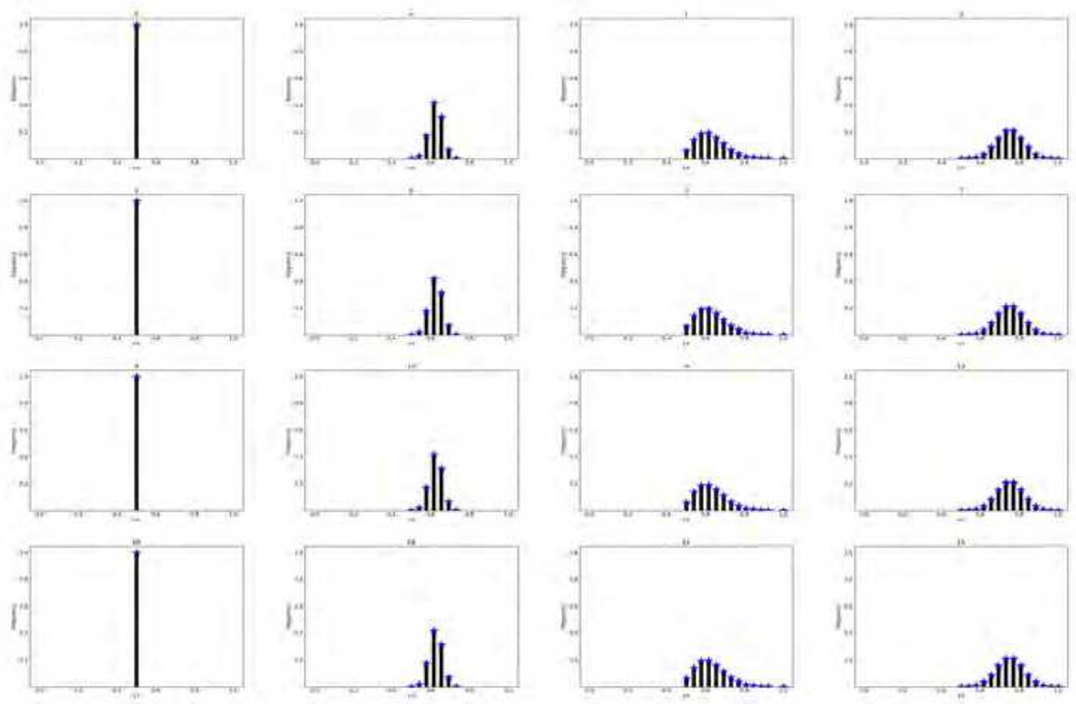

(e) Left

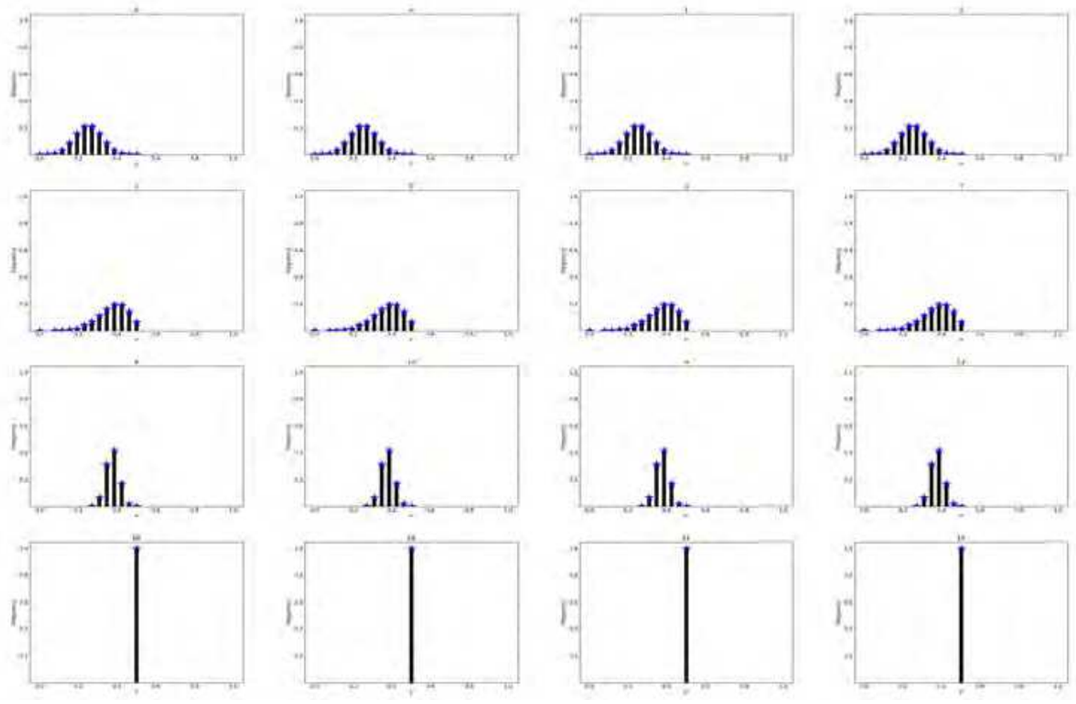

(f) Right

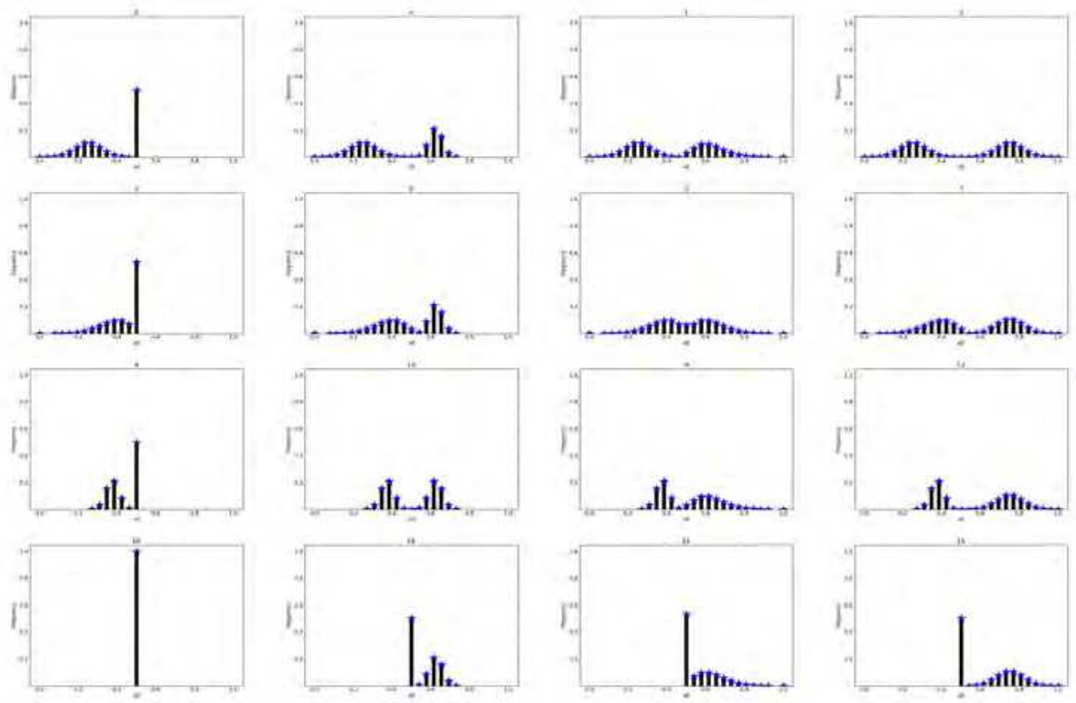

(g) D-P

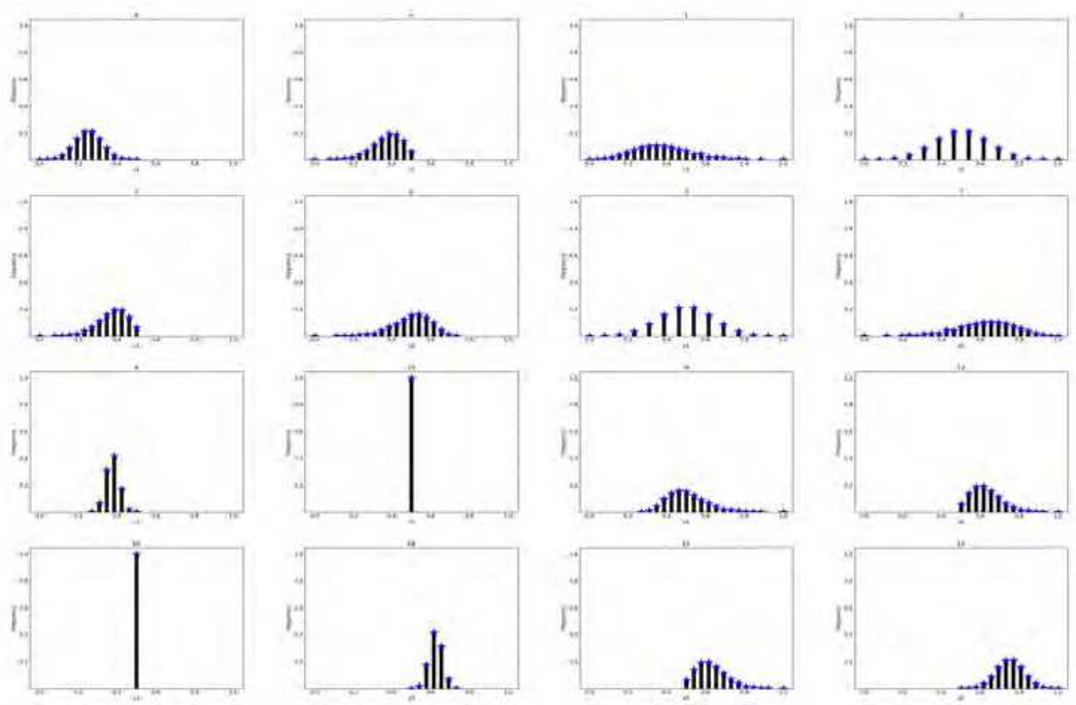

(h) D-W

Fig. 5. (a-h) Odd number groups: $N = \{13\}, f \in B_2^4$ Eight Matrices of Global Matrix Representations. (a) Left; (b) Right; (c) D-P; (d)D-W in symmetry conditions; (e) Left; (f) Right; (g) D-P; (h)D-W in anti-symmetry conditions.

Prediction 6: It will be much easier to design and implement key experiments to distinguish D-P and D-W behaviors in asynchronous conditions than in synchronous conditions.

In other words, under proposed variant measurements, the simplest effects are polarized properties in Left and Right matrices. Both D-P and D-W distributions are generated from pairs of polarized signals in general cases. In addition, significant differences can be observed between D-P and D-W distributions in asynchronous conditions. This set of theoretical predictions could help experimenters to design and implement effective experiments to check variant measurements under real quantum environments.

6.4 Two conjectures

Back to Young's waves and Newton's particles, Bohr's complementarity, EPR and Feynman's particle and wave conditions [Hawking & Mlodinow (2010); Jammer (1974); Penrose (2004)], it is essential to list two conjectures to summarize our results as follows:

Conjecture 1. Measurement results of Newton-Einstein-Feynman particles and Variant D-P models must obey Bell Inequations.

This conjecture could be approved from listed models satisfied independent conditions. From this viewpoint, Newton-Einstein-Feynman particle models and Variant D-P models could satisfy Bell Inequalities. Bell Inequations at most could provide only a logical foundation for different particle models.

Conjecture 2. Measurement results of Young-Bohr-Feynman waves and Variant D-W models satisfy the same types of entanglement conditions.

Since the Local Realism cannot be supported by quantum construction, a solid foundations is required to validate this conjecture using complex-probability conditions for different entanglements in real quantum environments.

7. Conclusion

Analyzing a N bit 0-1 vector and its exhaustive sequences for variant measurement, from a double path experiment viewpoint, this system simulates double path interference properties through different accurate distributions from local interactive measurements to global matrix representations. Using this model, two groups of parameters $\{u_\beta\}$ and $\{v_\beta\}$ describe left path, right path, and double paths for particles and double paths for waves with distinguishing symmetry and anti-symmetry properties. $\{P_H(u_\beta|J), P_H(v_\beta|J)\}$ provide eight groups of distributions under symmetry and anti-symmetry forms. In addition, $\{M(u_\beta), M(v_\beta)\}$ provide eight matrices to illustrate global behaviors under complex conditions.

Compared with the variant quaternion and other quaternion measurements, it is helpful to understand the usefulness and limitations of variant simulation properties.

The complexity of n-variable function space has a size of 2^{2^n} and exhaustive vector space has 2^N. Whole simulation complexity is determined by $O(2^{2^n} \times 2^N)$ as ultra exponent productions. How to overcome the limitations imposed by such complexity and how best to compare and contrast such simulations with real world experimentation will be key issues in future work.

Six predictions and two conjectures are summarized in this chapter to guide further theoretical and experimental exploration.

In addition, real world experiments are expected to be designed and implemented in the near future to test results given in this chapter.

8. Acknowledgements

Thanks to Colin W. Campbell for help with the English edition, to The School of Software Engineering, Yunnan University and The Key Laboratory of Yunnan Software Engineering for financial supports to the Information Security research projects (2010EI02, 2010KS06) and sub-CDIO project.

9. References

Afshar, S., Flores, E., McDonald, K. & Knoesel, E. (2007). Paradox in wave particle duality, *Found. Phys.* 37. 295-305.

Arndt, M., Nairz, O., Vos-Andreae, J., Keller, C., van der Zouw, G. & Zeilinger, A. (1999). Wave-particle duality of C60 molecules, *Nature* 401. 680-682.

Ash, R. B. & Doléans-Dade, C. A. (2000). *Probability & Measure Theory*, Elsevier.

Aspect, A. (2002). Bell's theorem: The naive view of an experimentalist, *Quatum [Un]speakables - From Bell to Quantum Information, Ed. Bertlmann and Zeilinger, Springer* .

Aspect, A., Grangier, P. & Roger, G. (1982). Experimental realization of einstein-podolsky-rosen-bohm gedankenexperiment: A new violation of bell's inequalities, *Phys. Rev. Lett.* 49. 91-94.

Barnett, S. M. (2009). *Quantum Information*, Oxford Uni. Press.

Barrow, J. D., Davies, P. C. W. & Charles L. Harper, J. E. (2004). *SCIENCE AND ULTIMATE REALITY: Quantum Theory, Cosmology and Complexity*, Cambridge University Press.

Bell, J. S. (1964). On the einstein-podolsky-rosen paradox, *Physics* 1. 195-200.

Bell, J. S. (2004). *Speakable and Unspeakable in Quantum Mechanics*, Cambridge Univ. Press.

Bohr, N. (1935). Can quantum-mechanical description of physical reality be considered complete?, *Physical Review* 48. 696-702.

Bohr, N. (1949). *Discussion with Einstein on Epistemological Problems in Atomic Physics*, Evanston. 200-241.

Clauser, J., Horne, N., Shimony, A. & Holt, R. (1969). Proposed experiment to test local hidden-variable theories, *PRL* 23. 880-884.

Cohn, E. G. D. (1990). George e. uhlenbeck and statistical mechanics, *Amer. J. Phys.* 58(7). 619-625.

de Broglie, L. (1923). Radiation, waves and quanta, *Comptes rendus* 177. 507-510.

Eberhard, P. (1978). Bell's theorem and the different concepts of locality, *Nuovo Cimento* 46B. 392-419.

Einstein, A. (1916). Strahlungs-emission und -absorption nach der Quantentheorie, *Verhandlungen der Deutschen Physikalischen Gesellschaft* 18. 318-323.

Einstein, A., Podolsky, B. & Rosen, N. (1935). Can quantum-mechanical description of physical reality be considered complete?, *Physical Review* 47. 770-780.

Feynman, R. (1965). *The Character of Physical Law*, MIT Press.

Feynman, R., Leighton, R. & Sands, M. (1965,1989). *The Feynman Lectures on Physics*, Vol. 3, Addison-Wesley, Reading, Mass.

Fine, A. (1999). Locality and the hardy theorem, *in From Physics to Philosophy, Cambridge University Press* .

Fox, M. (2006). *Quantum Optics*, Oxford Uni. Press.

Grangier, P., Roger, G. & Aspect, A. (1986). Experimental evidence for a photon anticorrelation effect on a beam splitter: A new light on single-photon interferences, *Europhys. Lett.* 1. 173-179.

Hawkingand, S. & Mlodinow, L. (2010). *The Grand Design*, Bantam Books.

Healey, R., Hellman, G. & Edited. (1998). *Quantum Measurement: Beyond Paradox*, Uni. Minnesota Press.

Jacques, V., Lai, N., Dréau, A., Zheng, D., Chauvat, D., Treussart, F., Grangier, P. & Roch, J. (2008). Illustration of quantum complementarity using single photons interfering on a grating, *New J. Phys.* 10. 123009, arXiv:0807.5079.

Jammer, M. (1974). *The Philosophy of Quantum Mechanics*, Wiley-Interscience Publication.

Lindner, F., Schätzel, M. G., Walther, H., Baltuska, A., Goulielmakis, E., Krausz, F., Milosevic, D. B., Bauer, D., Becker, W. & Paulus, G. G. (2005). Attosecond double-slit experiment, *Physical Review Letters* 95. 040401.

Merali, Z. (2007). Parallel universes make quantum sense, *New Scientist* 2622. http://space.newscientist.com/article/mg19526223.700-parallel-universes-make-quantum-sense.html.

Penrose, R. (2004). *The Road to Reality*, Vintage Books, London.

Schleich, W. P., Walther, H. & Edited (2007). *Elements of Quantum Information*, Wiley-VCH Verlag GmbH & Co KGaA Weinheim.

SEP (2009). Bell's theorem, *Stanford Encyclopedia of Philosophy* .
URL: *http://plato.stanford.edu/entries/bell-theorem/*

von Neumann, J. (1932,1996). *Mathematical Foundations of Quantum Mechanics*, Princeton Univ. Press.

Zeh, H. D. (1970). On the interpretation of measurement in quantum theory, *Foundation of Physics* 1. 69-76.

Zeilinger, A., Weihs, G., Jennewein, T. & Aspelmeyer, M. (2005). Happy centenary, photon, *Nature* 433. 230-238.

Zheng, J. (2011). Synchronous properties in quantum interferences, *Journal of Computations & Modelling, International Scientific Press* 1(1). 73-90.
URL: *http://www.scienpress.com/upload/JCM/Vol%201_1_6.pdf*

Zheng, J. & Zheng, C. (2010). A framework to express variant and invariant functional spaces for binary logic, *Frontiers of Electrical and Electronic Engineering in China, Higher Education Press and Springer* 5(2): 163–172.
URL: *http://www.springerlink.com/content/91474403127n446u/*

Zheng, J. & Zheng, C. (2011a). Variant measures and visualized statistical distributions, *Acta Photonica Sinica, Science Press* 40(9). 1397-1404. URL: *http://www.photon.ac.cn/CN /article/downloadArticleFile.do?attachType=PDF&id=15668*

Zheng, J. & Zheng, C. (2011b). Variant simulation system using quaternion structures, *Journal of Modern Optics, Taylor & Francis Group.* iFirst 1-9.
URL: *http://dx.doi.org/10.1080/09500340.2011.636152*

Zheng, J., Zheng, C. & Kunii, T. (2011). A framework of variant-logic construction for cellular automata, *Cellular Automata - Innovative Modelling for Science and Engineering edited Dr. A. Salcido, InTech Press*. 325-352. URL: *http://www.intechopen.com/articles/show/title/a-framework-of-variant-logic-construction-for-cellular-automata*

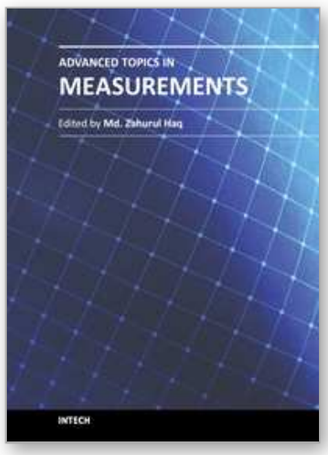

Advanced Topics in Measurements

Edited by Prof. Zahurul Haq

ISBN 978-953-51-0128-4
Hard cover, 400 pages
Publisher InTech
Published online 07, March, 2012
Published in print edition March, 2012

Measurement is a multidisciplinary experimental science. Measurement systems synergistically blend science, engineering and statistical methods to provide fundamental data for research, design and development, control of processes and operations, and facilitate safe and economic performance of systems. In recent years, measuring techniques have expanded rapidly and gained maturity, through extensive research activities and hardware advancements. With individual chapters authored by eminent professionals in their respective topics, Advanced Topics in Measurements attempts to provide a comprehensive presentation and in-depth guidance on some of the key applied and advanced topics in measurements for scientists, engineers and educators.

How to reference

In order to correctly reference this scholarly work, feel free to copy and paste the following:

Jeffrey Zheng, Christian Zheng and T.L. Kunii (2012). From Local Interactive Measurements to Global Matrix Representations on Variant Construction – A Particle Model of Quantum Interactions for Double Path Experiments, Advanced Topics in Measurements, Prof. Zahurul Haq (Ed.), ISBN: 978-953-51-0128-4, InTech, Available from: http://www.intechopen.com/books/advanced-topics-in-measurements/from-local-interactive-measurements-to-global-matrix-representations-on-variant-construction

InTech Europe
University Campus STeP Ri
Slavka Krautzeka 83/A
51000 Rijeka, Croatia
Phone: +385 (51) 770 447
Fax: +385 (51) 686 166
www.intechopen.com

InTech China
Unit 405, Office Block, Hotel Equatorial Shanghai
No.65, Yan An Road (West), Shanghai, 200040, China
中国上海市延安西路65号上海国际贵都大饭店办公楼405单元
Phone: +86-21-62489820
Fax: +86-21-62489821

© 2012 The Author(s). Licensee IntechOpen. This is an open access article distributed under the terms of the Creative Commons Attribution 3.0 License, which permits unrestricted use, distribution, and reproduction in any medium, provided the original work is properly cited.

IntechOpen

IntechOpen